

Charmed Λ_c^+ baryon decays into light scalar mesons in the topological $SU(3)_f$ framework

Y. L. Wang^{1,*} and Y. K. Hsiao^{1,†}

¹*School of Physics and Information Engineering,
Shanxi Normal University, Taiyuan 030031, China*

(Dated: May 28, 2025)

Abstract

Using the topological-diagram approach based on $SU(3)$ flavor symmetry, we investigate two-body $\Lambda_c^+ \rightarrow \mathbf{B}S$ decays, where Λ_c^+ is a member of the anti-triplet charmed baryons (\mathbf{B}_c), \mathbf{B} denotes a final-state baryon, and S refers to a light scalar meson, such as $f_0/f_0(980)$, $a_0/a_0(980)$, $\sigma_0/f_0(500)$, or $\kappa/K_0^*(700)$. Our analysis demonstrates that short-distance contributions, represented by the topological amplitudes, play a dominant role in these decays. In particular, this framework naturally accounts for the experimentally observed branching ratio $\mathcal{B}(\Lambda_c^+ \rightarrow \Lambda a_0^+)$, which exceeds predictions based solely on long-distance effects by an order of magnitude. Considering the light scalar mesons as tetraquark states, we predict $\mathcal{B}(\Lambda_c^+ \rightarrow pf_0, p\sigma_0) = (1.7 \pm 0.6, 0.02 \pm 0.01) \times 10^{-3}$ and $\mathcal{B}(\Lambda_c^+ \rightarrow \Sigma^+ f_0, \Sigma^+ \sigma_0) = (0.7 \pm 0.5, 1.5 \pm 0.7) \times 10^{-2}$. In addition, the decay $\Lambda_c^+ \rightarrow \Xi^0 \kappa^+$, which proceeds via a single W -exchange diagram, is found to have a branching fraction of $(4.9 \pm 0.9) \times 10^{-2}$. These results suggest that the branching ratios of $\mathbf{B}_c \rightarrow \mathbf{B}S$ are generally comparable to those of $\mathbf{B}_c \rightarrow \mathbf{B}M$, where M denotes a pseudoscalar meson. The predicted rates are sufficiently large to be probed in current experiments at BESIII, Belle II, and LHCb, offering promising opportunities to explore the internal structure of light scalar mesons.

* ylwang0726@163.com

† yukuohsiao@gmail.com

I. INTRODUCTION

Exotic multi-quark bound states, such as tetraquarks and pentaquarks, are predicted by the quark model to coexist with conventional mesons ($q\bar{q}$) and baryons (qqq) [1, 2]. However, the existence of charmless exotic states remains inconclusive. Among the most promising candidates for such states are the light scalar mesons (S): $f_0/f_0(980)$, $a_0/a_0(980)$, $\sigma_0/f_0(500)$, and $\kappa/K_0^*(700)$, with the masses below 1 GeV. These states are often proposed to possess a tetraquark structure, either as tightly bound (compact) $q^2\bar{q}^2$ states with gluon exchange [3–15], or as loosely bound meson-meson molecular states held together by residual strong force [16–23]. On the other hand, a conventional p-wave $q\bar{q}$ interpretation has not yet been definitively excluded [24–30]. To distinguish between these competing scenarios, extensive studies have been conducted in B -meson, D -meson, and b -baryon decays [31]. Curiously, however, investigations involving charmed baryon (\mathbf{B}_c) decays remain scarce.

Since the 1990 measurement of $\Lambda_c^+ \rightarrow pf_0$, which reported a branching fraction of $\mathcal{B}_{\text{ex}}(f_0) = (3.5 \pm 2.3) \times 10^{-3}$ [31, 32], no subsequent observations have been published for decays of $\mathbf{B}_c \rightarrow \mathbf{B}S$. Moreover, the large uncertainty associated with $\mathcal{B}_{\text{ex}}(f_0)$ casts doubt on the capability of charmed baryon decays to produce light scalar mesons with measurable rates. This seems to be broadly consistent with theoretical predictions, which estimate $\mathcal{B}(\mathbf{B}_c \rightarrow \mathbf{B}S) \simeq 10^{-5} - 10^{-4}$ [33], placing such decays near the edge of current experimental sensitivity. Nonetheless, renewed interest has been sparked by a potential resonant contribution in the decay $\Lambda_c^+ \rightarrow \Lambda(a_0^+ \rightarrow)\eta\pi^+$, suggested by the authors of Ref. [34]. This was motivated by a faint band, barely visible in the Dalitz plot of the Cabibbo-allowed process $\Lambda_c^+ \rightarrow \Lambda\eta\pi^+$ as reported by BELLE [35]. Although the structure was ultimately treated as a source of systematic uncertainty in the determination of $\mathcal{B}(\Lambda_c^+ \rightarrow \Lambda\eta\pi^+)$, its presence has nonetheless prompted further theoretical study, particularly incorporating final-state interactions (FSI) [34].

The FSI triangle rescattering mechanism has been applied to heavy hadron weak decays [34, 36–38]. In its extension [34], the weak decay $\Lambda_c^+ \rightarrow \Sigma^{*+}\eta$, with Σ^{*+} denoting the baryon decuplet $\Sigma(1385)^+$, is followed by the scattering of the Σ^{*+} with the η . Via the exchange of a charged pion, the Σ^{*+} can convert into a Λ , while the η transforms into an a_0^+ . By employing $SU(3)_f$ symmetry [39] and using the measured branching fraction $\mathcal{B}(\Lambda_c^+ \rightarrow \Sigma^{*+}\eta) = (1.21 \pm 0.04 \pm 0.10 \pm 0.06) \times 10^{-2}$ as input [35], we predict

$\mathcal{B}_{\text{th}}(a_0^+) \equiv \mathcal{B}(\Lambda_c^+ \rightarrow \Lambda a_0^+) = (1.7_{-1.0}^{+2.8} \pm 0.3) \times 10^{-3}$ [34]. This result constitutes the first theoretical estimate to reach the 10^{-3} level, providing strong motivation for future experimental verification.

Accordingly, the decay channels have been recently measured by BESIII, with the branching fractions reported as [40]

$$\begin{aligned}\mathcal{B}_{\text{ex}}(a_0^+) &\equiv \mathcal{B}(\Lambda_c^+ \rightarrow \Lambda a_0^+) = (1.23 \pm 0.21) \times 10^{-2}, \\ \mathcal{B}_{\text{ex}}(\Sigma^*) &\equiv \mathcal{B}(\Lambda_c^+ \rightarrow \Sigma^{*+} \eta) = (6.78 \pm 0.58 \pm 0.16 \pm 0.47) \times 10^{-3}.\end{aligned}\quad (1)$$

Both branching fractions exhibit intriguing discrepancies. First, $\mathcal{B}_{\text{ex}}(a_0)$ reaches the order of 10^{-2} , significantly exceeding the theoretical expectation. Second, the newly measured input $\mathcal{B}_{\text{ex}}(\Sigma^*)$, which is about half the value previously reported by BELLE, further reduces the predicted $\mathcal{B}_{\text{th}}(a_0^+)$ to be around 1×10^{-3} , making the discrepancy with $\mathcal{B}_{\text{ex}}(a_0^+)$ even more pronounced.

While $\mathcal{B}_{\text{th}}(a_0^+)$ could, in principle, be enhanced by an order of magnitude to match the experimental value, achieving this would require an overly arbitrary tuning of the cut-off parameter in the triangle-loop calculation. Other long-distance effects may contribute to the decay $\mathbf{B}_c \rightarrow \mathbf{B}S$ [33, 41–44]. In particular, both the pole model [33] and the rescattering mechanism [44] estimate $\mathcal{B}(\Lambda_c^+ \rightarrow \Lambda a_0^+)$ to be below 1×10^{-3} [40], and thus cannot account for $\mathcal{B}_{\text{ex}}(a_0^+)$ either.

As a possible resolution, we suggest that short-distance effects play a dominant role in $\mathbf{B}_c \rightarrow \mathbf{B}S$ decays, analogous to the well-established dominance in related processes such as $\mathbf{B}_c \rightarrow \mathbf{B}M$, where M denotes a pseudo-scalar meson. This resolution is further supported by experimental observations: the measured branching fractions $\mathcal{B}_{\text{ex}}(f_0)$ and $\mathcal{B}_{\text{ex}}(a_0^+)$ are found to be comparable in magnitude to $\mathcal{B}(\Lambda_c^+ \rightarrow p\eta') = (4.8 \pm 0.9) \times 10^{-4}$ and $\mathcal{B}(\Lambda_c^+ \rightarrow \Lambda\pi^+) = (1.29 \pm 0.05) \times 10^{-2}$, respectively [31]. This comparison is particularly relevant given that both f_0 and η' are expected to have significant $s\bar{s}$ content, while a_0 and π are members of the isospin triplet within the light scalar and pseudo-scalar nonets, respectively.

We therefore propose extending the the $SU(3)$ flavor $[SU(3)_f]$ -based topological-diagram approach (TDA), which has been successfully applied to heavy hadron decays [39, 45–54], to the analysis of $\mathbf{B}_c \rightarrow \mathbf{B}S$ processes. This framework will allows us to systematically examine whether the short-distance contributions, represented by topological diagrams, indeed dominate the decays, and to predict the branching fractions of potential decay channels.

Additionally, it offers a promising strategy to probe the internal structure of light scalar mesons, helping to determine whether they are conventional $q\bar{q}$ p-wave states or exotic $q^2\bar{q}^2$ tetraquark configurations.

II. FORMALISM

The effective Hamiltonian that governs the weak transition of the charm quark in the charmed baryon decays of $\mathbf{B}_c \rightarrow \mathbf{B}S$ is given by [55, 56]

$$\mathcal{H}_{eff} = \frac{G_F}{\sqrt{2}} V_{uq'} V_{cq}^* [c_1 (\bar{u}q')(\bar{q}c) + c_2 (\bar{u}_\beta q'_\alpha)(\bar{q}_\alpha c_\beta)], \quad (2)$$

where G_F is the Fermi constant, $c_{1,2}$ are the Wilson coefficients, and $V_{uq'} V_{cq}^*$ are the relevant Cabibbo-Kobayashi-Maskawa (CKM) matrix elements. Additionally, $(\bar{q}q') = \bar{q}\gamma_\mu(1 - \gamma_5)q'$ denotes the quark current, and the subscripts (α, β) are the color indices.

To facilitate the analysis within the framework of $SU(3)_f$ symmetry, we omit the Lorentz and color indices and express the Hamiltonian as $\mathcal{H}_c = \mathcal{H}_{eff}/(G_F/\sqrt{2}) = H_j^{ki}$, where the indices i, j , and k , ranging from 1 to 3, correspond to the light quark flavors (u, d, s). This tensor representation encodes the flavor transition $c \rightarrow q_i \bar{q}_j q_k$. The non-zero components of H_j^{ki} are [39, 45, 48, 49]

$$H_2^{31} = V_{cs}^* V_{ud}, \quad H_3^{31} = V_{cs}^* V_{us}, \quad H_2^{21} = V_{cd}^* V_{ud}, \quad H_3^{21} = V_{cd}^* V_{us}, \quad (3)$$

corresponding to the charm quark decays $c \rightarrow u\bar{d}s$, $u\bar{s}s$, $u\bar{d}d$, and $u\bar{s}d$, respectively. The associated CKM matrix elements are approximately given by $V_{cs}^* V_{ud} \simeq 1$, $V_{cs}^* V_{us} \simeq s_c$, $V_{cd}^* V_{ud} \simeq -s_c$, and $V_{cd}^* V_{us} \simeq -s_c^2$, where $s_c \equiv \sin \theta_c \simeq 0.22$, and θ_c is the Cabibbo angle. In the irreducible forms of $SU(3)_f$, the charmed baryon anti-triplet \mathbf{B}_c and the baryon octet \mathbf{B} are given by

$$\mathbf{B}_c = \begin{pmatrix} 0 & \Lambda_c^+ & \Xi_c^+ \\ -\Lambda_c^+ & 0 & \Xi_c^0 \\ -\Xi_c^+ & -\Xi_c^0 & 0 \end{pmatrix}, \quad \mathbf{B} = \begin{pmatrix} \frac{1}{\sqrt{6}}\Lambda^0 + \frac{1}{\sqrt{2}}\Sigma^0 & \Sigma^+ & p \\ \Sigma^- & \frac{1}{\sqrt{6}}\Lambda^0 - \frac{1}{\sqrt{2}}\Sigma^0 & n \\ \Xi^- & \Xi^0 & -\sqrt{\frac{2}{3}}\Lambda^0 \end{pmatrix}. \quad (4)$$

The light scalar final states, interpreted either as conventional $q\bar{q}$ p-wave mesons or as exotic $q^2\bar{q}^2$ tetraquark states, can be organized into two distinct irreducible representations under $SU(3)_f$ symmetry. In the $q\bar{q}$ configuration, the light scalar mesons S can be decomposed

as [7, 57]

$$\begin{aligned}
f_0 &= \cos \theta_I |s\bar{s}\rangle + \sin \theta_I |\sqrt{1/2}(u\bar{u} + d\bar{d})\rangle, \\
\sigma_0 &= -\sin \theta_I |s\bar{s}\rangle + \cos \theta_I |n\bar{n}\rangle, \\
a_0^+ &= |u\bar{d}\rangle, a_0^0 = |\sqrt{1/2}(u\bar{u} - d\bar{d})\rangle, a_0^- = |d\bar{u}\rangle, \\
\kappa^+ &= |u\bar{s}\rangle, \kappa^0 = |d\bar{s}\rangle, \bar{\kappa}^0 = |s\bar{d}\rangle, \kappa^- = |s\bar{u}\rangle,
\end{aligned} \tag{5}$$

where ϕ_I is the mixing angle in the $f_0 - \sigma_0$ mixing system. The Corresponding S nonet takes the form

$$S_{q\bar{q}} = \begin{pmatrix} \frac{1}{\sqrt{2}}(a_0^0 + c\phi_I\sigma_0 + s\phi_I f_0) & a_0^+ & \kappa^+ \\ a_0^- & \frac{-1}{\sqrt{2}}(a_0^0 - c\phi_I\sigma_0 - s\phi_I f_0) & \kappa^0 \\ \kappa^- & \bar{\kappa}^0 & -s\phi_I\sigma_0 + c\phi_I f_0 \end{pmatrix}, \tag{6}$$

with $(c\phi_I, s\phi_I) = (\cos \phi_I, \sin \phi_I)$. In the $q^2\bar{q}^2$ structure, the scalar mesons are instead described by [7]

$$\begin{aligned}
f_0 &= \cos \theta_{II} |\sqrt{1/2}(u\bar{u} + d\bar{d})s\bar{s}\rangle + \sin \theta_{II} |u\bar{u}d\bar{d}\rangle, \\
\sigma_0 &= -\sin \theta_{II} |\sqrt{1/2}(u\bar{u} + d\bar{d})s\bar{s}\rangle + \cos \theta_{II} |u\bar{u}d\bar{d}\rangle, \\
a_0^+ &= |u\bar{d}s\bar{s}\rangle, a_0^0 = |\sqrt{1/2}(u\bar{u} - d\bar{d})s\bar{s}\rangle, a_0^- = |d\bar{u}s\bar{s}\rangle, \\
\kappa^+ &= |u\bar{s}d\bar{d}\rangle, \kappa^0 = |d\bar{s}u\bar{u}\rangle, \bar{\kappa}^0 = |s\bar{d}u\bar{u}\rangle, \kappa^- = |s\bar{u}d\bar{d}\rangle,
\end{aligned} \tag{7}$$

where θ_{II} is the mixing angle in this scheme. The corresponding light scalar nonet is then given by

$$S_{q^2\bar{q}^2} = \begin{pmatrix} \frac{1}{\sqrt{2}}(a_0^0 + c\phi_{II}f_0 - s\phi_{II}\sigma_0) & a_0^+ & \kappa^+ \\ a_0^- & \frac{-1}{\sqrt{2}}(a_0^0 - c\phi_{II}f_0 + s\phi_{II}\sigma_0) & \kappa^0 \\ \kappa^- & \bar{\kappa}^0 & s\phi_{II}f_0 + c\phi_{II}\sigma_0 \end{pmatrix}, \tag{8}$$

with $(c\phi_{II}, s\phi_{II}) = (\cos \phi_{II}, \sin \phi_{II})$.

The decays $\mathbf{B}_c \rightarrow \mathbf{B}S$ proceed through various topological diagrams, as drawn in Fig. 1. Specifically, Figs. 1(a) and Figs. 1(b) illustrate the external and internal W -boson emission processes, denoted as T and C , respectively. These topologies involve the $\mathbf{B}_c \rightarrow \mathbf{B}$ transition, accompanied by the production of a light scalar meson from the vacuum. Fig. 1c shows the internal W -emission process labeled C' , which is non-factorizable. In Fig. 1(d), the topology labeled E' represents a W -boson exchange involving only the quark lines of the final-state

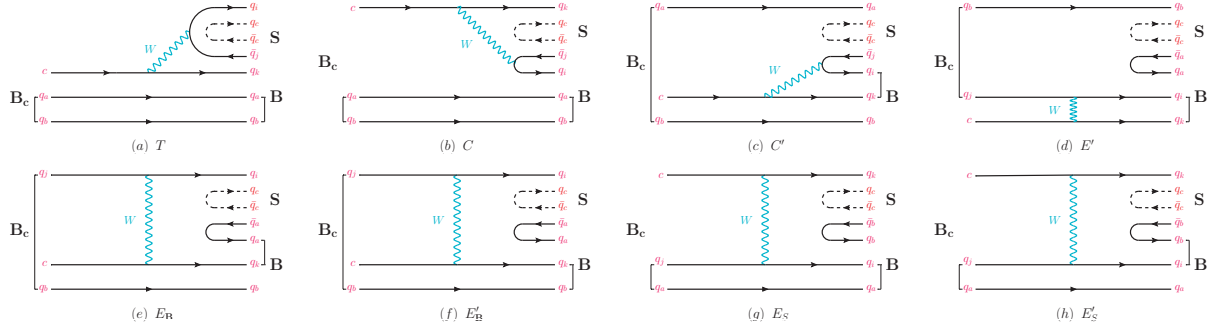


FIG. 1. Topological diagrams for $\mathbf{B}_c \rightarrow \mathbf{B}S$ decays are presented, featuring the possible inclusion of a $q_c \bar{q}_c$ pair within the $q^2 \bar{q}^2$ configuration of the light scalar meson S . Diagrams (a), (b), and (c) represent W -emission processes, while (d) through (h) correspond to W -exchange contributions. The notations “[” and “]” indicate the asymmetric quark orderings in the charmed baryon and octet baryon states, respectively.

baryon, without direct interaction with the quark contents of the light scalar meson. The diagrams labeled $E_{\mathbf{B}}$ in Fig. 1(e) and E_S in Fig. 1(g) illustrate W -exchange processes where the quark q_k , produced from the $c \rightarrow q_k$ transition, is incorporated into \mathbf{B} and S , respectively. The primed topologies, $E'_{\mathbf{B}}$ and E'_S , share the same overall structure as $E_{\mathbf{B}}$ and E_S , but differ in the specific anti-symmetric quark pair configuration within the baryon wave function.

Using the Hamiltonian components H_j^{ki} from Eq. (3) along with the irreducible forms of the initial and final states in Eqs. (4), (6), and (8), we construct the decay amplitudes for $\mathbf{B}_c \rightarrow \mathbf{B}S$ processes. This connection from the initial state \mathbf{B}_c to the final-state baryon \mathbf{B} and the light scalar meson S leads to the TDA amplitudes, expressed as [39, 45, 47, 49, 50, 52]

$$\begin{aligned}
\mathcal{M}_{\text{TDA}}(\mathbf{B}_c \rightarrow \mathbf{B}S) = & T \mathbf{B}_c^{ab} H_j^{ki} \mathbf{B}_{abk} S_j^i + C \mathbf{B}_c^{ab} H_j^{ki} \mathbf{B}_{abi} S_j^k + C' \mathbf{B}_c^{ab} H_j^{ki} \mathbf{B}_{ikb} S_j^a \\
& + E_{\mathbf{B}} \mathbf{B}_c^{jb} H_j^{ki} \mathbf{B}_{kab} S_a^i + E'_{\mathbf{B}} \mathbf{B}_c^{jb} H_j^{ki} \mathbf{B}_{kba} S_a^i \\
& + E_S \mathbf{B}_c^{jb} H_j^{ki} \mathbf{B}_{iba} S_a^k + E'_S \mathbf{B}_c^{jb} H_j^{ki} \mathbf{B}_{iab} S_a^k + E' \mathbf{B}_c^{jb} H_j^{ki} \mathbf{B}_{ika} S_a^b. \quad (9)
\end{aligned}$$

These terms correspond to the topological diagrams in Figs. 1(a)–(h), parameterized by the amplitudes $(T, C^{(\prime)}, E_{\mathbf{B}(S)}^{(\prime)}, E')$. The identity $\mathbf{B}_{ijk} = \epsilon_{ijl} \mathbf{B}_k^l$ has been used in the decomposition of the baryon octet. The full expansion of \mathcal{M}_{TDA} relates the decay amplitudes of various channels through the topological parameters. Both the $q\bar{q}$ and $q^2 \bar{q}^2$ configurations of the light scalar mesons S are considered in this analysis. In the expansion, the combination $(E' - E'_{\mathbf{B}})$ consistently appears, indicating redundancy. Therefore, we simplify the

amplitude structure by setting $E'_{\mathbf{B}} = 0$. The amplitudes carry prefactors of s_c^0 , s_c^1 , and s_c^2 , corresponding to Cabibbo-allowed (CA), singly Cabibbo-suppressed (SCS), and doubly Cabibbo-suppressed (DCS) decays, respectively, in the $\mathbf{B}_c \rightarrow \mathbf{B}S$ processes.

According to the measurements, the branching fractions $\mathcal{B}_{\text{ex}}(f_0) \simeq \mathcal{B}(\Lambda_c^+ \rightarrow p\eta')$ and $\mathcal{B}_{\text{ex}}(a_0^+) \simeq \mathcal{B}(\Lambda_c^+ \rightarrow \Lambda\pi^+)$ suggest that $\mathcal{B}(\mathbf{B}_c \rightarrow \mathbf{B}S)$ can be as significant as $\mathcal{B}(\mathbf{B}_c \rightarrow \mathbf{B}M)$, even though most of them have yet to be directly observed. Nonetheless, the branching fractions for the resonant processes $\mathcal{B}(\mathbf{B}_c \rightarrow \mathbf{B}S, S \rightarrow MM)$ are accessible experimentally. Among the measured total branching fractions for $\mathbf{B}_c \rightarrow \mathbf{B}MM$ decays [31], we highlight $\mathcal{B}_T(\Lambda_c^+ \rightarrow \Sigma^+\pi^+\pi^-, \Sigma^+K^+K^-) = (44.7 \pm 2.2, 3.59 \pm 0.35) \times 10^{-3}$, which are clearly much larger than the non-resonant components $\mathcal{B}_{\text{NR}}(\Lambda_c^+ \rightarrow \Sigma^+\pi^+\pi^-, \Sigma^+K^+K^-) = (28.0 \pm 5.0, 0.46 \pm 0.04) \times 10^{-3}$, as investigated in [69, 76]. In addition, known resonant contributions include $\mathcal{B}_V(\Lambda_c^+ \rightarrow \Sigma^+\rho^0, \rho^0 \rightarrow \pi^+\pi^-) = (4.5 \pm 2.3) \times 10^{-3}$, $\mathcal{B}_V(\Lambda_c^+ \rightarrow \Sigma^+\phi, \phi \rightarrow K^+K^-) = (2.0 \pm 0.3) \times 10^{-3}$, and $\mathcal{B}_{\mathbf{B}^*}(\Lambda_c^+ \rightarrow \Sigma^{*0}\pi^+, \Sigma^{*0} \rightarrow \Sigma^+\pi^-) = (0.36 \pm 0.05) \times 10^{-3}$, updated from the analyses in Refs. [39, 70]. These values are obtained using the approximations for resonant branching fractions

$$\begin{aligned}\mathcal{B}_V &\equiv \mathcal{B}(\mathbf{B}_c \rightarrow \mathbf{B}V, V \rightarrow MM) \simeq \mathcal{B}(\mathbf{B}_c \rightarrow \mathbf{B}V) \times \mathcal{B}(V \rightarrow MM), \\ \mathcal{B}_{\mathbf{B}^*} &\equiv \mathcal{B}(\mathbf{B}_c \rightarrow \mathbf{B}^*M, \mathbf{B}^* \rightarrow \mathbf{B}M) \simeq \mathcal{B}(\mathbf{B}_c \rightarrow \mathbf{B}^*M) \times \mathcal{B}(\mathbf{B}^* \rightarrow \mathbf{B}M),\end{aligned}\quad (10)$$

with $\mathcal{B}(\rho^0 \rightarrow \pi^+\pi^-) \simeq 1$, $\mathcal{B}(\phi \rightarrow K^+K^-) = (49.1 \pm 0.5) \times 10^{-2}$, and $\mathcal{B}(\Sigma^{*0} \rightarrow \Sigma^+\pi^-) = (5.85 \pm 0.75) \times 10^{-2}$ [31]. Using the relation $\mathcal{B}_T = \mathcal{B}_S + \mathcal{B}_V + \mathcal{B}_{\mathbf{B}^*} + \mathcal{B}_{\text{NR}}$, we extract the scalar meson resonance contributions as follows

$$\begin{aligned}\mathcal{B}_S(f_0, a_0^0) &\equiv \mathcal{B}(\Lambda_c^+ \rightarrow \Sigma^+(f_0 \rightarrow)K^+K^- + \Sigma^+(a_0^0 \rightarrow)K^+K^-) = (1.13 \pm 0.46) \times 10^{-3}, \\ \mathcal{B}_S(f_0, \sigma_0) &\equiv \mathcal{B}(\Lambda_c^+ \rightarrow \Sigma^+(f_0 \rightarrow)\pi^+\pi^- + \Sigma^+(\sigma_0 \rightarrow)\pi^+\pi^-) = (11.6 \pm 6.0) \times 10^{-3}.\end{aligned}\quad (11)$$

Consequently, the values $\mathcal{B}_{\text{ex}}(f_0)$, $\mathcal{B}_{\text{ex}}(a_0^+)$, $\mathcal{B}_S(f_0, a_0^0)$, and $\mathcal{B}_S(f_0, \sigma_0)$ constitute four experimental inputs in our analysis.

At present, the four experimental inputs are insufficient to constrain all topological parameters. To enable a practical global fit, a reduction in the number of free parameters is necessary. In this context, the equivalence between the topological-diagram approach (TDA) and the irreducible representation approach (IRA) based on $SU(3)_f$ symmetry proves particularly useful. The IRA formalism introduces a set of symmetry-based parameters within the amplitudes \mathcal{M}_{IRA} , which are equally applicable to describing charmed baryon decays

TABLE I. Topological amplitudes of $\Lambda_c^+ \rightarrow \mathbf{B}a_0, \mathbf{B}\kappa$.

Decay mode	$\mathcal{M}_{q\bar{q}} = \mathcal{M}_{q^2\bar{q}^2}$
$\Lambda_c^+ \rightarrow \Lambda^0 a_0^+$	$-\frac{1}{\sqrt{6}}(4T + C' - E_{\mathbf{B}} - E')$
$\Lambda_c^+ \rightarrow \Sigma^0 a_0^+$	$\frac{1}{\sqrt{2}}(C' + E_{\mathbf{B}} - E')$
$\Lambda_c^+ \rightarrow \Sigma^+ a_0^0$	$-\frac{1}{\sqrt{2}}(C' + E_{\mathbf{B}} - E')$
$\Lambda_c^+ \rightarrow \Xi^0 \kappa^+$	E'
$\Lambda_c^+ \rightarrow p \bar{\kappa}^0$	$2C - E'_S$
$\Lambda_c^+ \rightarrow \Lambda^0 \kappa^+$	$[-\frac{1}{\sqrt{6}}(4T + C' - E_{\mathbf{B}} + E')]s_c$
$\Lambda_c^+ \rightarrow \Sigma^0 \kappa^+$	$[\frac{1}{\sqrt{2}}(C' + E_{\mathbf{B}})]s_c$
$\Lambda_c^+ \rightarrow \Sigma^+ \kappa^0$	$(-E'_S + C')s_c$
$\Lambda_c^+ \rightarrow n a_0^+$	$(-2T - C' + E')s_c$
$\Lambda_c^+ \rightarrow p a_0^0$	$[\frac{1}{\sqrt{2}}(2C - C' - E_{\mathbf{B}} - E'_S + E')]s_c$
$\Lambda_c^+ \rightarrow p \kappa^0$	$(C' - 2C)s_c^2$
$\Lambda_c^+ \rightarrow n \kappa^+$	$-(C' + 2T)s_c^2$

 TABLE II. Topological amplitudes of $\Lambda_c^+ \rightarrow \mathbf{B}f_0, \mathbf{B}\sigma_0$ in the $f_0 - \sigma_0$ mixing scheme.

Decay mode	$\mathcal{M}_{q\bar{q}}$	$\mathcal{M}_{q^2\bar{q}^2}$
$\Lambda_c^+ \rightarrow \Sigma^+ f_0$	$\frac{1}{\sqrt{2}}(C' - E_{\mathbf{B}} + E')s\phi_I + E'_S c\phi_I$	$\frac{1}{\sqrt{2}}(C' - E_{\mathbf{B}} + E')c\phi_{II} + E'_S s\phi_{II}$
$\Lambda_c^+ \rightarrow \Sigma^+ \sigma_0$	$\frac{1}{\sqrt{2}}(C' - E_{\mathbf{B}} + E')c\phi_I - E'_S s\phi_I$	$-\frac{1}{\sqrt{2}}(C' - E_{\mathbf{B}} + E')s\phi_{II} + E'_S c\phi_{II}$
$\Lambda_c^+ \rightarrow p f_0$	$[-\frac{1}{\sqrt{2}}(2C - C' - E'_S + E_{\mathbf{B}} - E')s\phi_I + 2C c\phi_I]s_c$	$[-\frac{1}{\sqrt{2}}(2C - C' - E'_S + E_{\mathbf{B}} - E')c\phi_{II} + 2C s\phi_{II}]s_c$
$\Lambda_c^+ \rightarrow p \sigma_0$	$[-\frac{1}{\sqrt{2}}(2C - C' - E'_S + E_{\mathbf{B}} - E')c\phi_I - 2C s\phi_I]s_c$	$[\frac{1}{\sqrt{2}}(2C - C' - E'_S + E_{\mathbf{B}} - E')s\phi_{II} + 2C c\phi_{II}]s_c$

as those in the TDA framework, \mathcal{M}_{TDA} [58–75]. Crucially, it has been shown that the two approaches are equivalent, with the relation $\mathcal{M}_{\text{TDA}} = \mathcal{M}_{\text{IRA}}$ established in several studies [39, 48, 49, 51, 52, 54]. As a result, the TDA parameters can be related to one another through their correspondence with the IRA parameters. Given that the topological amplitudes for $\mathbf{B}_c \rightarrow \mathbf{B}S$ are nearly identical to those for $\mathbf{B}_c \rightarrow \mathbf{B}M$, aside from differences arising from the f_0 – σ_0 mixing schemes, the established equivalence relations from the $\mathbf{B}_c \rightarrow \mathbf{B}M$ analysis [48] are applicable here. Accordingly, we adopt the relation $E'_S = E_{\mathbf{B}}$ in our study.

Factorization also contributes to the reduction of parameters. The TDA amplitudes T and C correspond to factorizable external and internal W -boson emission processes, respectively. These contributions can be expressed as $\mathcal{M}_{\text{fac}} \propto \langle S | (\bar{u}q') | 0 \rangle \langle \mathbf{B} | (\bar{q}c) | \mathbf{B}_c \rangle$. Due to the parameterization of $\langle S | (\bar{u}q') | 0 \rangle = f_S q^\mu$, where the decay constant f_S can be zero or very small [86, 87], $\mathcal{M}_{\text{fac}} \simeq 0$. As a result, we obtain $T = C \simeq 0$.

While all currently available data points arise from Λ_c^+ decays, we focus our analysis on the $\Lambda_c^+ \rightarrow \mathbf{B}S$ decay channels. The corresponding TDA amplitudes are explicitly listed in Tables I and II. Considering the reductions $T = C = E'_{\mathbf{B}} = 0$ and the equivalence relation

$E'_S = E_{\mathbf{B}}$, the remaining topological parameters relevant to $\Lambda_c^+ \rightarrow \mathbf{B}S$ decays are

$$C', E', E_{\mathbf{B}}. \quad (12)$$

The amplitude E_S , which contributes only to $\Xi_c^0 \rightarrow \mathbf{B}S$ decays, is excluded from this study.

III. NUMERICAL ANALYSIS

In our numerical analysis, we adopt the value $s_c = \lambda = 0.22453 \pm 0.00044$ from the PDG [31], where λ denotes the Wolfenstein parameter. For the $f_0 - \sigma_0$ mixing, two scenarios are considered. In the $q\bar{q}$ configuration, the mixing angle θ_I is taken as a weighted average of values extracted from multiple studies [15, 30, 77–84]. In the alternative $q^2\bar{q}^2$ configuration, the mixing angle θ_{II} is taken from Ref. [7]. These angles are given by

$$\begin{aligned} \theta_I &= (156.7 \pm 0.7)^\circ, \\ \theta_{II} &= (174.6^{+3.4}_{-3.2})^\circ. \end{aligned} \quad (13)$$

We employ a minimum χ^2 fit defined as

$$\chi^2 = \sum_i \left(\frac{\mathcal{B}_{\text{th}}^i - \mathcal{B}_{\text{ex}}^i}{\sigma_{\text{ex}}^i} \right)^2, \quad (14)$$

where \mathcal{B}_{th} is the theoretical branching fraction computed as $\mathcal{B}_{\text{th}} = (G_F^2 |\vec{p}_{\mathbf{B}}| \tau_{\Lambda_c}) / (16\pi m_{\Lambda_c}^2) \times |\mathcal{M}(\Lambda_c^+ \rightarrow \mathbf{B}S)|^2$. Here, $\mathcal{M}(\Lambda_c^+ \rightarrow \mathbf{B}S)$ is the topological amplitudes from Tables I and II, and τ_{Λ_c} and m_{Λ_c} denote the lifetime and mass of Λ_c^+ , respectively. The three-momentum of the final-state baryon in the Λ_c^+ rest frame is given by $|\vec{p}_{\mathbf{B}}| = [(m_{\Lambda_c}^2 - m_+^2)(m_{\Lambda_c}^2 - m_-^2)]^{1/2} / (2m_{\Lambda_c})$, with $m_{\pm} = m_{\mathbf{B}} \pm m_S$.

In Eq. (14), we use $\mathcal{B}_{\text{ex}}(f_0)$, $\mathcal{B}_{\text{ex}}(a_0^+)$, $\mathcal{B}_S(f_0, a_0^0)$, and $\mathcal{B}_S(f_0, \sigma_0)$ as the experimental inputs \mathcal{B}_{ex} , with their respective uncertainties σ_{ex} . Notably, $\mathcal{B}_S(f_0, a_0^0)$ and $\mathcal{B}_S(f_0, \sigma_0)$ are extracted from three-body decay measurements. To account for this, we use the approximation $\mathcal{B}_S \equiv \mathcal{B}(\mathbf{B}_c \rightarrow \mathbf{B}S, S \rightarrow MM) \simeq \mathcal{B}(\mathbf{B}_c \rightarrow \mathbf{B}S) \times \mathcal{B}(S \rightarrow MM)$, analogous to the treatment in Eq. (10). The scalar meson decay branching fractions used in the analysis are $\mathcal{B}(f_0 \rightarrow \pi^+\pi^-, K^+K^-) = (0.49, 0.13)$ [85], $\mathcal{B}(\sigma_0 \rightarrow \pi^+\pi^-) = 0.67$ [86, 87], and $\mathcal{B}(a_0^0 \rightarrow K^+K^-) = 0.075$ [86, 87]. These inputs allow us to include the theoretical branching ratios $\mathcal{B}_{\text{th}}(\Lambda_c^+ \rightarrow \Sigma^+ f_0, \Sigma^+ a_0^0)$ and $\mathcal{B}_{\text{th}}(\Lambda_c^+ \rightarrow \Sigma^+ f_0, \Sigma^+ \sigma_0)$ in the numerical analysis.

TABLE III. Branching fractions of $\mathbf{B}_c \rightarrow \mathbf{B}S$ calculated within the topological-diagram approach, where the uncertainties reflect those propagated from the mixing angles in Eq. (13) and the fitted topological parameters in Eq. (15).

Branching fraction	This work: (S1, S2)	Data
$10^2 \mathcal{B}(\Lambda_c^+ \rightarrow \Lambda^0 a_0^+)$	$(1.2 \pm 0.5, 1.2 \pm 0.4)$	1.23 ± 0.21 [40]
$10^2 \mathcal{B}(\Lambda_c^+ \rightarrow \Sigma^0 a_0^+)$	$(0.01 \pm 0.12, 0.4 \pm 0.4)$	
$10^2 \mathcal{B}(\Lambda_c^+ \rightarrow \Sigma^+ a_0^0)$	$(0.01 \pm 0.12, 0.4 \pm 0.4)$	
$10^2 \mathcal{B}(\Lambda_c^+ \rightarrow \Xi^0 \kappa^+)$	$(3.1 \pm 1.1, 4.9 \pm 0.9)$	
$10^2 \mathcal{B}(\Lambda_c^+ \rightarrow p \bar{\kappa}^0)$	$(2.7 \pm 1.0, 1.2 \pm 0.8)$	
$10^2 \mathcal{B}(\Lambda_c^+ \rightarrow \Sigma^+ f_0)$	$(0.9 \pm 0.5, 0.7 \pm 0.5)$	
$10^2 \mathcal{B}(\Lambda_c^+ \rightarrow \Sigma^+ \sigma_0)$	$(1.2 \pm 0.9, 1.5 \pm 0.7)$	
$10^3 \mathcal{B}(\Lambda_c^+ \rightarrow \Lambda^0 \kappa^+)$	$(0.7 \pm 0.5, 1.6 \pm 0.6)$	3.4 ± 2.3 [31, 32]
$10^3 \mathcal{B}(\Lambda_c^+ \rightarrow \Sigma^0 \kappa^+)$	$(0.8 \pm 0.5, 0.4 \pm 0.4)$	
$10^3 \mathcal{B}(\Lambda_c^+ \rightarrow \Sigma^+ \kappa^0)$	$(0.8 \pm 0.8, 0.3 \pm 0.5)$	
$10^3 \mathcal{B}(\Lambda_c^+ \rightarrow n a_0^+)$	$(1.4 \pm 1.0, 2.3 \pm 1.1)$	
$10^3 \mathcal{B}(\Lambda_c^+ \rightarrow p a_0^0)$	$(0.4 \pm 0.6, 0.01 \pm 0.14)$	
$10^3 \mathcal{B}(\Lambda_c^+ \rightarrow p f_0)$	$(0.2 \pm 0.1, 1.7 \pm 0.6)$	
$10^3 \mathcal{B}(\Lambda_c^+ \rightarrow p \sigma_0)$	$(1.5 \pm 0.8, 0.02 \pm 0.01)$	
$10^5 \mathcal{B}(\Lambda_c^+ \rightarrow p \bar{\kappa}^0)$	$(0.2 \pm 1.3, 0.2 \pm 1.3)$	
$10^5 \mathcal{B}(\Lambda_c^+ \rightarrow n \kappa^+)$	$(0.2 \pm 1.3, 0.2 \pm 1.3)$	

By performing a global fit under two scenarios S1 and S2, corresponding to $S_{q\bar{q}}$ in Eq. (6) and $S_{q^2\bar{q}^2}$ in Eq. (8), respectively, we extract the topological parameters as follows

$$\begin{aligned}
\text{S1 : } & (C', E', E_{\mathbf{B}}) = (0.08 \pm 0.14, 0.64 \pm 0.11, 0.50 \pm 0.09) \text{ GeV}^3, \\
\text{S2 : } & (C', E', E_{\mathbf{B}}) = (0.08 \pm 0.14, 0.81 \pm 0.07, 0.34 \pm 0.09) \text{ GeV}^3.
\end{aligned} \tag{15}$$

The goodness of the fit is quantified by χ^2 of 2.0 for S1 and 0.6 for S2. The number of degrees of freedom (n.d.f) is 1 in both cases. Based on the fitted parameters in Eq.(15), the predicted branching fractions $\mathcal{B}(\Lambda_c^+ \rightarrow \mathbf{B}S)$ are presented in Table III.

IV. DISCUSSIONS AND CONCLUSION

Within the $SU(3)_f$ framework, the decay channels of $\Lambda_c^+ \rightarrow \mathbf{B}S$ are systematically analyzed, with the $SU(3)_f$ topological parameters employed to relate the amplitudes across all possible decay modes. Due to the limited experimental data, specifically, $\mathcal{B}_{\text{ex}}(f_0)$, $\mathcal{B}_{\text{ex}}(a_0^+)$, $\mathcal{B}_S(f_0, a_0^0)$, and $\mathcal{B}_S(f_0, \sigma_0)$, this study focuses exclusively on the decays $\Lambda_c^+ \rightarrow \mathbf{B}S$. The successful global fits to the available data indicates that short-distance contributions, as

captured by the topological diagrams, play a dominant role in governing the $\Lambda_c^+ \rightarrow \mathbf{B}S$ processes.

As factorization leads to $T = C \simeq 0$, the branching fractions are expected to be dominated by non-factorizable topological contributions. As shown in the fit results of Eq. (15), C' is small, while E' and $E_{\mathbf{B}}$ are significant in both scenarios. Consequently, the Cabibbo-allowed amplitudes can be approximated as $\mathcal{M}(\Lambda_c^+ \rightarrow \Lambda a_0^+) \simeq \frac{1}{\sqrt{6}}(E_{\mathbf{B}} + E')$ and $\mathcal{M}(\Lambda_c^+ \rightarrow \Sigma^{0(+)} a_0^{+(0)}) \simeq \frac{1}{\sqrt{2}}(E_{\mathbf{B}} - E')$, where constructive interference occurs for $\Lambda_c^+ \rightarrow \Lambda a_0^+$, and destructive interference for $\Lambda_c^+ \rightarrow \Sigma^{0(+)} a_0^{+(0)}$. The resulting branching fractions are

$$\begin{aligned}\mathcal{B}_{q\bar{q}}(\Lambda_c^+ \rightarrow \Lambda^0 a_0^+, \Sigma^{0(+)} a_0^{+(0)}) &= (1.2 \pm 0.5, 0.01 \pm 0.12) \times 10^{-2}, \\ \mathcal{B}_{q^2\bar{q}^2}(\Lambda_c^+ \rightarrow \Lambda^0 a_0^+, \Sigma^{0(+)} a_0^{+(0)}) &= (1.2 \pm 0.4, 0.4 \pm 0.4) \times 10^{-2},\end{aligned}\quad (16)$$

where $\mathcal{B}_{q\bar{q}, q^2\bar{q}^2}$ correspond to the cases where S is treated as the $q\bar{q}$ and $q^2\bar{q}^2$ states, respectively. The suppression of $\Lambda_c^+ \rightarrow \Lambda^0 a_0^+$ compared to $\Lambda_c^+ \rightarrow \Sigma^{0(+)} a_0^{+(0)}$ arises from the interference pattern in each scenario. Both theoretical results for $\Lambda_c^+ \rightarrow \Lambda^0 a_0^+$ are consistent with $\mathcal{B}_{\text{ex}}(a_0^+) \simeq 10^{-2}$, suggesting that this mode is not sensitive to the internal structure of a_0 . In contrast, a precise measurement of $\mathcal{B}(\Lambda_c^+ \rightarrow \Sigma^{0(+)} a_0^{+(0)}) \sim 4 \times 10^{-3}$ or its deviation from this value could help discriminate between the $q\bar{q}$ and $q^2\bar{q}^2$ structures of the light scalar meson.

We also predict the following branching fractions

$$\begin{aligned}\mathcal{B}_{q\bar{q}}(\Lambda_c^+ \rightarrow \Sigma^+ f_0, \Sigma^+ \sigma_0) &= (0.9 \pm 0.5, 1.2 \pm 0.9) \times 10^{-2}, \\ \mathcal{B}_{q^2\bar{q}^2}(\Lambda_c^+ \rightarrow \Sigma^+ f_0, \Sigma^+ \sigma_0) &= (0.7 \pm 0.5, 1.5 \pm 0.7) \times 10^{-2}.\end{aligned}\quad (17)$$

These results show that, in both the S1 and S2 scenarios, the branching fractions of $\Lambda_c^+ \rightarrow \mathbf{B}S$ decays can reach the 10^{-3} to 10^{-2} level, making them accessible to future experimental measurements. Short-distance contributions are responsible for producing several branching fractions as large as 10^{-2} . For instance, the decays $\Lambda_c^+ \rightarrow \Xi^0 \kappa^+$ and $\Lambda_c^+ \rightarrow p \bar{\kappa}^0$ receive exclusive contributions from E' and $-E'_S$ (equivalently $-E_{\mathbf{B}}$), respectively. As a result, we predict $\mathcal{B}_{(q\bar{q}, q^2\bar{q}^2)}(\Lambda_c^+ \rightarrow \Xi^0 \kappa^+) = (3.1 \pm 1.1, 4.9 \pm 0.9) \times 10^{-2}$ and $\mathcal{B}_{(q\bar{q}, q^2\bar{q}^2)}(\Lambda_c^+ \rightarrow p \bar{\kappa}^0) = (2.7 \pm 1.0, 1.2 \pm 0.8) \times 10^{-2}$. It is worth noting that the analogous decays $\Lambda_c^+ \rightarrow \Xi^0 K^+, \Xi^{*0} K^+$, which proceed via a single E' contribution, have the measured branching fractions of approximately 5×10^{-3} [88]. This highlights that generally all $\mathbf{B}_c \rightarrow \mathbf{B}S$ decays can naturally

attain branching fractions comparable to those of $\mathbf{B}_c \rightarrow \mathbf{B}M$, supporting the expectation of significant rates in many of these channels.

In the $q\bar{q}$ picture, $s\phi_I^2 \simeq 0.016$ in $\mathcal{B}_{q\bar{q}}(\Lambda_c^+ \rightarrow pf_0) \propto s\phi_I^2 \times (E')^2$ results in a significantly suppressed branching fraction. Consequently, we obtain $\mathcal{B}_{q\bar{q}}(\Lambda_c^+ \rightarrow pf_0) = (0.15 \pm 0.08) \times 10^{-3}$, which is about 20 times smaller than the experimental value of $(3.4 \pm 2.3) \times 10^{-3}$ [31, 32]. By contrast, in the $q^2\bar{q}^2$ tetraquark scenario, $c\phi_{II}^2 \simeq 1.0$ in $\mathcal{B}_{q^2\bar{q}^2}(\Lambda_c^+ \rightarrow pf_0) \propto c\phi_{II}^2 \times (E')^2$ leads to $\mathcal{B}_{q^2\bar{q}^2}(\Lambda_c^+ \rightarrow pf_0) = (1.7 \pm 0.6) \times 10^{-3}$, which is in reasonable agreement with the data. The quality of the fits reflects this difference. In the S1 global fit, $\chi^2/n.d.f = 2.0$ indicates a poor match to the experimental data, whereas $\chi^2/n.d.f = 0.6$ in the S2 global fit is close to 1, suggesting a better overall consistency. This mild preference lends some support to the tetraquark interpretation.

According to the mild preference with $\chi^2/n.d.f$, currently the measured branching fractions remains insufficient and not precise enough to confirm the quark contents of light scalar mesons. In particular, the uncertainty in $\mathcal{B}_{\text{ex}}(f_0)$ remains sizeable, highlighting the need for further investigation. To aid future analysis, we identify the following relations

$$\begin{aligned} \frac{\mathcal{B}_{q\bar{q}}(\Lambda_c^+ \rightarrow pf_0)}{\mathcal{B}_{q\bar{q}}(\Lambda_c^+ \rightarrow p\sigma_0)} &= \tan^2 \theta_I \times (\Phi_{f_0}/\Phi_{\sigma_0}) = 0.127, \\ \frac{\mathcal{B}_{q^2\bar{q}^2}(\Lambda_c^+ \rightarrow p\sigma_0)}{\mathcal{B}_{q^2\bar{q}^2}(\Lambda_c^+ \rightarrow pf_0)} &= \tan^2 \theta_{II} \times (\Phi_{\sigma_0}/\Phi_{f_0}) = 0.015, \end{aligned} \quad (18)$$

where $\tan^2 \theta_I = 0.19$, $\tan^2 \theta_{II} = 0.01$, and $(\Phi_{f_0}/\Phi_{\sigma_0}) = 0.67$ denotes the ratio of the integrated phase space factors defined below Eq. (14). Notably, these ratios are independent of the topological parameters and their uncertainties. Hence, future experimental efforts can test the contrasting relations: $\mathcal{B}_{q\bar{q}}(\Lambda_c^+ \rightarrow pf_0) \simeq 0.1\mathcal{B}_{q\bar{q}}(\Lambda_c^+ \rightarrow p\sigma_0)$ and $\mathcal{B}_{q^2\bar{q}^2}(\Lambda_c^+ \rightarrow p\sigma_0) \simeq 0.02\mathcal{B}_{q^2\bar{q}^2}(\Lambda_c^+ \rightarrow pf_0)$, which may provide a clear signature to distinguish between the two scenarios.

In summary, we have proposed that short-distance contributions, captured by the topological diagrams within the $SU(3)_f$ framework, play a dominant role in $\mathbf{B}_c \rightarrow \mathbf{B}S$. Using the current experimental data, we extracted the relevant topological amplitudes and applied them to compute branching fractions across various decay channels. Our analysis successfully accounted for the observed branching fraction of $\Lambda_c^+ \rightarrow \Lambda a_0^+$, which is measured to be an order of magnitude larger than predictions based solely on long-distance effects. By modeling the light scalar mesons as tetraquark candidates, we showed that the

branching fractions of $\Lambda_c^+ \rightarrow \mathbf{B}S$ can be comparable to those of $\Lambda_c^+ \rightarrow \mathbf{B}M$, driven predominantly by non-factorizable short-distance contributions. In particular, we predicted $\mathcal{B}(\Lambda_c^+ \rightarrow pf_0) = (1.7 \pm 0.6) \times 10^{-3}$, $\mathcal{B}(\Lambda_c^+ \rightarrow \Sigma^+ f_0, \Sigma^+ \sigma_0) = (0.7 \pm 0.5, 1.5 \pm 0.7) \times 10^{-2}$, and a substantially suppressed $\mathcal{B}(\Lambda_c^+ \rightarrow p\sigma_0) = (0.02 \pm 0.01) \times 10^{-3}$. We also found that the decay $\Lambda_c^+ \rightarrow \Xi^0 \kappa^+$, which receives a sole contribution from a non-factorizable W -exchange diagram, yields $\mathcal{B}(\Lambda_c^+ \rightarrow \Xi^0 \kappa^+) = (4.9 \pm 0.9) \times 10^{-2}$. Additionally, we have performed global fits under the assumption that light scalar mesons are conventional $q\bar{q}$ states. While this scenario can still accommodate the data, it yields a slightly larger $\chi^2/n.d.f$ compared to the tetraquark interpretation, indicating that the $q^2\bar{q}^2$ picture is somewhat more favored by current measurements.

ACKNOWLEDGMENTS

This work was supported in parts by National Science Foundation of China (Grants No. 12175128 and No. 11675030).

-
- [1] M. Gell-Mann, Phys. Lett. **8**, 214 (1964).
 - [2] G. Zweig, CERN-TH-412 (CERN) 1964.
 - [3] R. L. Jaffe, Phys. Rev. D **15**, 267 (1977).
 - [4] R. L. Jaffe, Phys. Rev. D **15**, 281 (1977).
 - [5] F. E. Close and N. A. Tornqvist, J. Phys. G **28**, R249 (2002).
 - [6] J. R. Pelaez, Phys. Rev. Lett. **92**, 102001 (2004).
 - [7] L. Maiani, F. Piccinini, A. D. Polosa and V. Riquer, Phys. Rev. Lett. **93**, 212002 (2004).
 - [8] C. Amsler and N. A. Tornqvist, Phys. Rept. **389**, 61 (2004).
 - [9] R. L. Jaffe, Phys. Rept. **409**, 1 (2005).
 - [10] N. N. Achasov and A. V. Kiselev, Phys. Rev. D **73**, 054029; erratum: **74**, 059902 (2006).
 - [11] G. 't Hooft, G. Isidori, L. Maiani, A. D. Polosa and V. Riquer, Phys. Lett. B **662**, 424 (2008).
 - [12] A. H. Fariborz, R. Jora and J. Schechter, Phys. Rev. D **79**, 074014 (2009).
 - [13] S. Weinberg, Phys. Rev. Lett. **110**, 261601 (2013).
 - [14] S. S. Agaev, K. Azizi and H. Sundu, Phys. Lett. B **789**, 405 (2019).

- [15] Y. K. Hsiao, S. Q. Yang, W. J. Wei and B. C. Ke, JHEP **12**, 226 (2025).
- [16] J. D. Weinstein and N. Isgur, Phys. Rev. D **41**, 2236 (1990).
- [17] V. Baru, J. Haidenbauer, C. Hanhart, Y. Kalashnikova and A. E. Kudryavtsev, Phys. Lett. B **586**, 53 (2004).
- [18] L. Y. Dai and M. R. Pennington, Phys. Lett. B **736**, 11 (2014).
- [19] T. Branz, T. Gutsche and V. E. Lyubovitskij, Eur. Phys. J. A **37**, 303 (2008).
- [20] D. L. Yao, L. Y. Dai, H. Q. Zheng and Z. Y. Zhou, Rept. Prog. Phys. **84**, 076201 (2021).
- [21] L. Y. Dai, X. G. Wang and H. Q. Zheng, Commun. Theor. Phys. **58**, 410 (2012).
- [22] T. Sekihara and S. Kumano, Phys. Rev. D **92**, 034010 (2015).
- [23] Z. Q. Wang, X. W. Kang, J. A. Oller and L. Zhang, Phys. Rev. D **105**, 074016 (2022).
- [24] V. V. Anisovich, V. A. Nikonov and L. Montanet, Phys. Lett. B **480**, 19 (2000).
- [25] I. Bediaga, F. S. Navarra and M. Nielsen, Phys. Lett. B **579**, 59 (2004).
- [26] T. M. Aliev and M. Savci, EPL **90**, 61001 (2010).
- [27] P. Colangelo, F. De Fazio and W. Wang, Phys. Rev. D **81**, 074001 (2010).
- [28] Y. J. Shi and W. Wang, Phys. Rev. D **92**, 074038 (2015).
- [29] N. R. Soni, A. N. Gadaria, J. J. Patel and J. N. Pandya, Phys. Rev. D **102**, 016013 (2020).
- [30] E. Klempt, Phys. Lett. B **820**, 136512 (2021).
- [31] S. Navas *et al.* (Particle Data Group), Phys. Rev. D **110**, 030001 (2024).
- [32] S. Barlag *et al.* [ACCMOR], Z. Phys. C **48**, 29 (1990).
- [33] A. Sharma and R.C. Verma, J. Phys. G **36**, 075005 (2009).
- [34] Y. Yu and Y. K. Hsiao, Phys. Lett. B **820**, 136586 (2021).
- [35] J. Y. Lee *et al.* [Belle Collaboration], Phys. Rev. D **103**, 052005 (2021).
- [36] Y. K. Hsiao, Y. Yu and B. C. Ke, Eur. Phys. J. C **80**, 895 (2020).
- [37] Y. Yu, Y. K. Hsiao and B. C. Ke, Eur. Phys. J. C **81**, 1093 (2021).
- [38] Y. K. Hsiao, S. T. Cai and Y. L. Wang, Phys. Rev. D **111**, 076020 (2025).
- [39] Y. K. Hsiao, Q. Yi, S. T. Cai and H. J. Zhao, Eur. Phys. J. C **80**, 1067 (2020).
- [40] M. Ablikim *et al.* [BESIII], Phys. Rev. Lett. **134**, 021901 (2025).
- [41] J. J. Xie and L. S. Geng, Eur. Phys. J. C **76**, 496 (2016).
- [42] Z. Wang, Y. Y. Wang, E. Wang, D. M. Li and J. J. Xie, Eur. Phys. J. C **80**, 842 (2020).
- [43] X. C. Feng, L. L. Wei, M. Y. Duan, E. Wang and D. M. Li, Phys. Lett. B **846**, 138185 (2023).

- [44] G. Y. Wang, N. C. Wei, H. M. Yang, E. Wang, L. S. Geng and J. J. Xie, Phys. Rev. D **106**, 056001 (2022).
- [45] J. Pan, Y. K. Hsiao, J. Sun and X. G. He, Phys. Rev. D **102**, 056005 (2020).
- [46] Y. K. Hsiao, JHEP **11**, 117 (2023).
- [47] H. J. Zhao, Y. L. Wang, Y. K. Hsiao and Y. Yu, JHEP **02**, 165 (2020).
- [48] Y. K. Hsiao, Y. L. Wang and H. J. Zhao, JHEP **09**, 035 (2022).
- [49] Y. L. Wang, H. J. Zhao and Y. K. Hsiao, Phys. Rev. D **111**, 016022 (2025).
- [50] Y. Kohara, Phys. Rev. D **44**, 2799 (1991).
- [51] X. G. He and W. Wang, Chin. Phys. C **42**, 103108 (2018).
- [52] X. G. He, Y. J. Shi and W. Wang, Eur. Phys. J. C **80**, 359 (2020).
- [53] D. Wang, C. P. Jia and F. S. Yu, JHEP **21**, 126 (2020).
- [54] H. Y. Cheng, F. Xu and H. Zhong, Phys. Rev. D **111**, 034011 (2025).
- [55] G. Buchalla, A. J. Buras and M. E. Lautenbacher, Rev. Mod. Phys. **68**, 1125 (1996).
- [56] A.J. Buras, hep-ph/9806471.
- [57] S. Stone and L. Zhang, Phys. Rev. Lett. **111**, 062001 (2013).
- [58] D. Zeppenfeld, Z. Phys. C **8**, 77 (1981).
- [59] M. J. Savage and R. P. Springer, Phys. Rev. D **42**, 1527 (1990).
- [60] M. J. Savage, Phys. Lett. B **257**, 414 (1991).
- [61] K. K. Sharma and R. C. Verma, Phys. Rev. D **55**, 7067 (1997).
- [62] C. D. Lu, W. Wang and F. S. Yu, Phys. Rev. D **93**, 056008 (2016).
- [63] C. Q. Geng, Y. K. Hsiao, C. W. Liu and T. H. Tsai, JHEP **1711**, 147 (2017).
- [64] C. Q. Geng, Y. K. Hsiao, Y. H. Lin and L. L. Liu, Phys. Lett. B **776**, 265 (2017).
- [65] C. Q. Geng, Y. K. Hsiao, C. W. Liu and T. H. Tsai, Eur. Phys. J. C **78**, 593 (2018).
- [66] C. Q. Geng, Y. K. Hsiao, C. W. Liu and T. H. Tsai, Phys. Rev. D **97**, 073006 (2018).
- [67] D. Wang, P. F. Guo, W. H. Long and F. S. Yu, JHEP **03**, 066 (2018).
- [68] D. Wang, Eur. Phys. J. C **79**, 429 (2019).
- [69] C. Q. Geng, Y. K. Hsiao, C. W. Liu and T. H. Tsai, Phys. Rev. D **99**, 073003 (2019).
- [70] Y. K. Hsiao, Y. Yu and H. J. Zhao, Phys. Lett. B **792**, 35 (2019).
- [71] C. P. Jia, D. Wang and F. S. Yu, Nucl. Phys. B **956**, 115048 (2020).
- [72] F. Huang, Z. P. Xing and X. G. He, JHEP **03**, 143 (2022).
- [73] D. Wang, JHEP **12**, 003 (2022).

- [74] Z. P. Xing, X. G. He, F. Huang and C. Yang, Phys. Rev. D **108**, 053004 (2023).
- [75] H. Zhong, F. Xu, Q. Wen and Y. Gu, JHEP **02**, 235 (2023).
- [76] C. Q. Geng, C. W. Liu and S. L. Liu, Phys. Rev. D **109**, 093002 (2024).
- [77] W. Ochs, J. Phys. G **40**, 043001 (2013).
- [78] J. W. Li, D. S. Du and C. D. Lu, Eur. Phys. J. C **72**, 2229 (2012).
- [79] R. Aaij *et al.* [LHCb], Phys. Rev. D **92**, 032002 (2015).
- [80] A. V. Anisovich *et al.* [SIGMA-AYAKS], Phys. Atom. Nucl. **65**, 497 (2002).
- [81] C. Di Donato, G. Ricciardi and I. Bigi, Phys. Rev. D **85**, 013016 (2012).
- [82] P. Minkowski and W. Ochs, Eur. Phys. J. C **9**, 283 (1999).
- [83] A. V. Sarantsev, I. Denisenko, U. Thoma and E. Klempt, Phys. Lett. B **816**, 136227 (2021).
- [84] F. L. Braghin, J. Phys. G **50**, 095101 (2023).
- [85] L. L. Mu and X. Q. Yu, Phys. Rev. D **111**, 016002 (2025).
- [86] H. Y. Cheng, Phys. Rev. D **67**, 034024 (2003).
- [87] H. Y. Cheng, C. W. Chiang and Z. Q. Zhang, Phys. Rev. D **105**, 033006 (2022).
- [88] M. Ablikim *et al.* [BESIII], Phys. Lett. B **783**, 200 (2018).